Available online at www.sciencedirect.com
SCIENCE DIRECT
Journal of Applied Geophysics 58 (2006) 218–231
JOURNAL OF APPLIED GEOPHYSICS
www.elsevier.com/locate/jappgeo

A comparison of different radiomagnetotelluric data inversion methods for buried waste sites

M.E. Candansayar [a,*], B. Tezkan [b]

[a] Ankara University, Faculty of Engineering, Department of Geophysical Engineering, 06100, Ankara, Turkey
[b] University of Cologne, Institute of Geophysics and Meteorology, Germany

Received 25 June 2003; accepted 25 June 2005

Abstract

This study deals with two-dimensional (2D) inversions of synthetic and observed radiomagnetotelluric (RMT) data on typical buried conductive waste sites in Europe, and with the practical aspects of different inversion algorithms. In the inversion calculations, we used smoothing and L2-norm stabilizers and compared the results. The resolution of the geometry of the highly conductive waste site, in particular, was investigated. In the inversion with the L2-norm stabilizer, we used the least-squares solution with singular value decomposition (LSSVD) and conjugate gradient (CG), whereas only the conjugate gradient solver was used in the 2D-inversion with the smoothing stabilizer. The inversion results of the synthetic data showed a better resolution of the geometry of the highly conductive waste site when a L2-norm stabilizer was applied in the inversion; in particular, a better detection of the bottom of the waste deposit was achieved. Additional model studies were carried out using synthetic RMT data in order to investigate the 2D inversion of RMT data observed on a 3D structure; these studies showed that the use of TM mode data yields a better resolution of the structure than joint inversion of TE and TM modes.

2D inversions of RMT data on a waste site near Cologne showed that the inversion of the TM mode could resolve well the geometry, especially the bottom of the waste site, if information about the background conductivity structure was available. In this case study, inversion with the L2-norm stabilizer produced a sharper image of the waste site than inversion with the smoothing stabilizer, as indicated also by the inversion study that used synthetic data.

Keywords: Radiomagnetotelluric; 2D inversion; Waste site; Smoothing stabilizer; The L2-norm stabilizer

1. Introduction

The RMT method is an extension of the well-known Very-Low-Frequency (VLF) technique to higher frequencies. RMT uses radio transmitters in a frequency range between 10 to 300 kHz with a possible extension to 1 MHz. The RMT method has been

* Corresponding author. Tel.: +90 312 212 67 20x13 71; fax: +90 312 212 00 71.
E-mail address: candansa@eng.ankara.edu.tr (M.E. Candansayar).

0926-9851/$ - see front matter © 2005 Elsevier B.V. All rights reserved.
doi:10.1016/j.jappgeo.2005.07.001

used with increasing popularity for ground-water research (Turberg et al., 1994; Beamish, 2000), waste-site studies (Zacher et al., 1996a; Tezkan et al., 1996, 2000), and archaeological investigations (Zacher et al., 1996b; Baum, 1998).

The RMT method has proven quite efficient in waste-site studies. However, it is sometimes difficult to resolve the bottom of waste deposits from the 2D inversion of the observed scalar RMT data — the main reasons being the three-dimensionality of the structure and/or screening effects of the highly conductive anomaly due to the limited frequency range of the RMT method. However, possible 3D effects on RMT data cannot be studied using scalar RMT data acquisition. In addition, the smoothing stabilizer that has been used in inversion algorithms to date (e.g., Tezkan, 1999; Tezkan et al., 2000; Newman et al., 2003) may be another reason. Therefore, two different inversion approaches (the L2 norm of model parameters and the Laplacian norm of model parameters) are compared for models of typical buried, conductive waste sites in order to study the effects of the smoothing stabilizer.

RMT data are usually collected for frequency pairs of radio transmitters situated roughly parallel and perpendicular to the assumed strike direction of a 2D conductivity structure. The RMT method uses carrier waves from high-powered civilian and military transmitters that operate in a frequency range between 10 kHz and 1 MHz. Local electromagnetic fields can be assumed to be of plane waves (McNeill and Labson, 1991) because of the great distance (>8 times skin depth) between the survey area and such transmitters (vertical electric dipole). The EM field consists of a horizontal magnetic field perpendicular to the direction of propagation and a horizontal electric field in the direction of propagation. Model calculations also show that displacement currents can be neglected in central Europe under normal conditions (expected resistivities of less than 1000 Ω m) up to 1 MHz, and the plane-wave assumption is valid for RMT data (Schröder, 1994). Therefore, magnetotelluric (MT) inversion algorithms can be used for RMT data interpretation (e.g., Beamish, 1994, 2000; Tezkan et al., 2000). RMT data acquisition is rapid in comparison to traditional MT measurements. However, RMT data are usually acquired in scalar mode in most applications. Bastani (2001) and Bastani and Pedersen (2001) introduced a newly developed RMT system that performs tensor measurements. Apparent resistivities and phases in scalar mode are measured parallel and perpendicular to polarization directions, which are associated – in the case of a 2D anomaly – with a known strike direction relative to the TE (transverse electric – electric field parallel to the strike direction) and TM (transverse magnetic – magnetic field parallel to the strike direction) modes.

RMT data are usually interpreted using 2D inversion calculations. The 2D inversion codes used for the interpretation of RMT data (e.g., Beamish, 1994, 2000; Tezkan et al., 2000) are OCCAM (deGroot-Hedlin and Constable, 1990) and D2INV (Mackie et al., 1997; Rodi and Mackie, 2001). OCCAM uses the finite element algorithm, PW2D (Wannamaker et al., 1987), for forward calculations, the sensitivity-equation approach (McGillivray et al., 1994) for the Jacobian (frechet derivative or sensitivity) matrix calculation, and the least-squares solution with singular value decomposition (LSSVD) for the inverse calculation. In the code D2INV, the forward calculation is done by using the transmission-network analog of Madden (1972), and the Jacobian matrix is calculated by the adjoint-equation approach (McGillivray et al., 1994) in which the reciprocity principle is employed and the nonlinear conjugate gradient (NLCG) algorithm is used in the inverse procedure. The codes, OCCAM and D2INV, use the Laplacian norm of the model parameters as a stabilizer (smoothing inversion) in the inversion algorithm. Hence, 2D smooth inversion of RMT data at times can mask the main target structure, such as the bottom of a waste site. In such cases, different algorithms using different stabilizers, such as the L2 norm of the model parameter vector, may give more accurate results than smoothing inversion.

Candansayar (2002a,b) developed a new code, named regularized 2D magnetotelluric inversion (R2DMTINV). He compared results of 2D inversions of M‘T data using CG and LSSVD algorithms with different stabilizers with this code. He suggested that a consecutive use of LSSVD and CG algorithms (LSSVD_CG) with the L2-norm stabilizer generates more accurate results than the single use of each algorithm. Forward calculations are made by using the finite difference method, and the adjoint-equation

approach is used for the calculation of the Jacobian matrix in the code. CG and LSSVD inversion algorithms can also be used separately or consecutively in this code.

Synthetic data and field data observed on a waste site are used to compare different inversion results by utilizing CG, LSSVD, and LSSVD_CG (which use the L2 norm of the model parameter as a stabilizer) algorithms with the inversion code, R2DMTINV, and NLCG (which uses the Laplacian norm of model parameters as a stabilizer) algorithms with the inversion code, D2INV. The main difference between the CG and NLCG algorithms is that the former uses the L2 norm of the model parameters as a stabilizer, whereas the latter uses the Laplacian norm of the model parameters as a stabilizer. Below we show that the L2-norm stabilizer approach is sometimes superior to the smoothing stabilizer.

2. 2D inversion

The electromagnetic inverse problem which is solved with some regularization methods is nonlinear and ill-posed. The following parametric functional is minimized (Tikhonov and Arsenin, 1977) in the regularization

$$P(\boldsymbol{m},\boldsymbol{d}) = \varphi(\boldsymbol{m},\boldsymbol{d}) + \alpha S(\boldsymbol{m}) = \min \tag{1}$$

where $\varphi(\boldsymbol{m},\boldsymbol{d})$ and $S(\boldsymbol{m})$ are the misfit functional and the stabilizer (stabilizing functional or model objective functional), respectively. α is a regularization parameter (penalty parameter) that is a real number. $\varphi(\boldsymbol{m},\boldsymbol{d})$ may be defined as the L2 norm of the vector consisting of calculated and measured data differences,

$$\varphi_{\mathrm{w}}(\boldsymbol{m},\boldsymbol{d}) = \left\|\mathbf{W}_{\mathrm{d}} f(\boldsymbol{m}) - \mathbf{W}_{\mathrm{d}}\boldsymbol{d}\right\|^2 \tag{2}$$

where f is the forward operator, $\boldsymbol{d}$ is the data vector $N\times 1$ consisting of the logarithm of apparent resistivity in ohm meters and phase of impedance in radians for each frequency, $\boldsymbol{m}$ is the $M\times 1$ model vector that consists of the logarithm of unknown block resistivities, and $\mathbf{W}_{\mathrm{d}}$ is the diagonal weighting matrix with elements that are reciprocals of the error estimates of the observed data.

The well-known stabilizer is based on the least-squares criterion or, in other words, on the L2 norm of the model parameter vector defined as

$$S_{\mathrm{L}_2}(\boldsymbol{m}) = \left\|\boldsymbol{m}\right\|^2_{\mathrm{L}_2} = \min. \tag{3}$$

Minimization of Eq. (1) with this stabilizer (with respect to the parameters and the solution of the resulting equation) is known as the dumped least-squares (or Levenberg–Marquardt) inverse solution (Meju, 1994). The Laplacian norm of the model parameters is another stabilizer commonly used in the 2D inversion of electromagnetic data. It is called a "smoothing stabilizer" and is given as (Rodi and Mackie, 2001)

$$S_{\mathrm{Sm}}(\boldsymbol{m}) = \left\|\nabla^2\boldsymbol{m}\right\|^2 = \left(\nabla^2\boldsymbol{m}, \nabla^2\boldsymbol{m}\right) = \min \tag{4}$$

where ∇^2 is the Laplacian operator. In practice, it is a second-order derivative matrix. Inversion with this stabilizer is called smoothing (or OCCAM) inversion and generates smoother models (Sasaki, 1989; deGroot-Hedlin and Constable, 1990).

Using Eqs. (2) and (3) in (1), we get

$$P(\boldsymbol{m},\boldsymbol{d}) = \left\|\mathbf{W}_{\mathrm{d}} f(\boldsymbol{m}) - \mathbf{W}_{\mathrm{d}}\boldsymbol{d}\right\|^2 + \alpha\left\|\boldsymbol{m}\right\|^2 \tag{5}$$

and, similarly, Eqs. (2) and (4) in Eq. (1),

$$P(\boldsymbol{m},\boldsymbol{d}) = \left\|\mathbf{W}_{\mathrm{d}} f(\boldsymbol{m}) - \mathbf{W}_{\mathrm{d}}\boldsymbol{d}\right\|^2 + \alpha\left\|\nabla^2\boldsymbol{m}\right\|^2. \tag{6}$$

The parametric functionals, (5) and (6), are commonly solved by using either the least squares with singular value decomposition (LSSVD) or with the nonlinear conjugate gradient (CG or NLCG) algorithms, as presented in Candansayar (2002a) and Rodi and Mackie (2001), respectively. These solvers have both advantages and drawbacks. Candansayar (2002b) suggested a consecutive use of the two solvers (called LSSVD_CG solution) in order to gain the advantages of each solution.

The regularization parameter α controls a trade off between the misfit and the stabilizer and is of vital importance in the estimation of this value. However, there is no unique approach for selecting α. In the preliminary nonlinear inverse problem in electromagnetic methods, α was found after several trials and this constant value is used as a fixed parameter in further iterations (e.g., Sasaki, 1989). However, the resolution in the inversion can be improved by adjusting the value of α at each iteration. Nowadays, as a standard

approach, an initial α is selected as a large value due to the large misfit of the initial model. Subsequently, it is gradually reduced in the following iterations in a nonlinear regularized inversion. This approach is known as "cooling approximation" and is used by many researchers (e.g. Zhang and Hobbs, 1992; LaBrecque et al., 1997; Newman and Hoversten, 2000; Farquharson and Oldenburg, 1998, 2004). The same approximation is used in both codes, R2DMTINV and D2INV. Thus, we selected an optimum α in order to give a reasonable data residual and to minimize the parametric functional in each algorithm.

In this study, the CG, LSSVD and LSSVD_CG solution of the Eq. (5) and the NLCG solution (smoothing inversion) of Eq. (6) are tested on the RMT data. In all algorithms, the iteration stops when the model can no longer be improved. The final models are represented with the number of iterations and the misfit values calculated as follows

$$\mathrm{MISFIT} = \left(\sum_{i=1}^{N}(\boldsymbol{d}_i - f(\boldsymbol{m})_i^2\right)^{1/2} \Big/ \left(\sum_{i=1}^{N}\boldsymbol{d}_i^2\right)^{1/2} \tag{7}$$

where N is the number of data, $\boldsymbol{d}_i$ and $f(\boldsymbol{m})_i$ are i-th measured and calculated data, respectively.

3. 2D inversion of synthetic and field data

Two synthetic-data sets and one field-data set were used in order to compare the resolution capacity of the CG, LSSVD, LSSVD_CG and NLCG algorithms. The solution of Eq. (5) is realized by using CG, LSSVD, and LSSVD_CG algorithms for synthetic data and the LSSVD_CG algorithm for field data. On the other hand, smoothing inversion (the solution of Eq. (6)) is realized by using the NLCG algorithm (Mackie et al., 1997) for synthetic and field data.

The grids used for the inversion of the synthetic and field data are constructed according to the rules given by Wannamaker et al. (1987), which are based on skin-depth information. It should also be taken into account that the grids used for inversion of the synthetic data coincide with the mesh of the block boundaries of the original model and represent the ideal case for the application of different inversion algorithms.

4. Inversion of synthetic data

4.1. First model

A synthetic data set was generated at 27 points for frequencies 234, 126, 53, and 18.3 kHz, by using the finite element modeling algorithm developed by Wannamaker et al. (1987). These frequencies are typically used for RMT surveys near Cologne. The model used is a simple waste site (Fig. 1a). The background geology is represented by a three-layer earth model with resistivities of 50, 500, and 25 Ω m, respectively, from top to bottom. The corresponding thicknesses of these layers are assumed to be 2 and 20 m, respectively. The conductive body, representing the waste pit with a 20 Ω m resistivity, is located at a depth between 3–13 m (Fig. 1a). A 5% Gaussian noise was added to the data before inversion. The spacing of the stations was 10 m for stations away from the conductive target, 5 m for stations near the target, and 2.5 m for stations close to the boundary between the conductive target and the surrounding medium. This is a typical RMT field setup for waste-site surveys. A 120 Ω m homogenous half-space was used as the initial model in all calculations. The selected resistivity is an average of the generated apparent resistivities at all stations and all frequencies. The real and estimated models from the joint inversion of TE-and TM-mode data are shown in Fig. 1.

The numbers of iterations and data misfits are given in the figure for each model. The regularization parameter α was determined by using the cooling approximation (Newman and Hoversten, 2000; Candansayar, 2002a,b) in the code R2DMTINV (for CG, LSSVD and LSSVD_CG algorithms). Hence, the 2D models in Fig. 1b and c were calculated for $\alpha = 0.53$. The D2INV code (NLCG algorithm) was executed several times by using different values of α to find the optimal data misfit. The 2D model presented in Fig. 1e was calculated for the $\alpha = 20$ value by using the NLCG algorithm. In general, the lateral and vertical borders of the conductive structure representing the waste pollution were resolved by all inversion algorithms. However, the first layer could not be resolved accurately by any estimated model due to the lack of higher RMT frequencies. The NLCG algorithm generated a smooth model as expected (Fig. 1e). The bottom of the conductive body was

located at a depth of 13 ms (Fig. 1a), and it was resolved more sharply by the LSSVD_CG (Fig. 1d). The LSSVD_CG algorithm shows the minimum data misfit and number of iterations.

The central depth of the in-phase induced currents, z^*, (Schmuckher, 1987) was used as a guide for the maximum depth from which information about the conductivity structure could be obtained. z^* is defined as

$$z^* = \sqrt{\frac{\rho_a}{\omega\mu_0}}\sin\phi$$

where ρ_a is the apparent resistivity in ohm meters, ϕ is the impedance phase in degrees, ω is the angular frequency ($\omega = 2\pi f$, f is frequency), and μ_0 is the permeability of free space. Ziebell (1997) showed that $2z^*$ can be used for RMT frequencies for the maximum interpretation depth in the case of waste-site surveys (Tezkan et al., 2000). VLF frequencies were used for the determination of the maximum depth ($2z^*$ values on the waste site), which is about 26 m for 18.3 kHz for the 2D model in Fig. 1a. The model calculations of Ziebell (1997) also showed that the vertical gradient of resistivity in a 2D conductive waste model should be greater than 6 Ω m/m in order to resolve layers from each other. This condition is also validated by all 2D conductivity models in Fig. 1. The minimum vertical resistivity gradient between the blocks at the bottom of the conductive target and the surrounding medium is 16 Ω m/m for the model derived by the NLCG inversion, and 48 Ω m/m for the model derived by the LSSVD_CG inversion. These are the maximum values of all estimated models, and they indicate

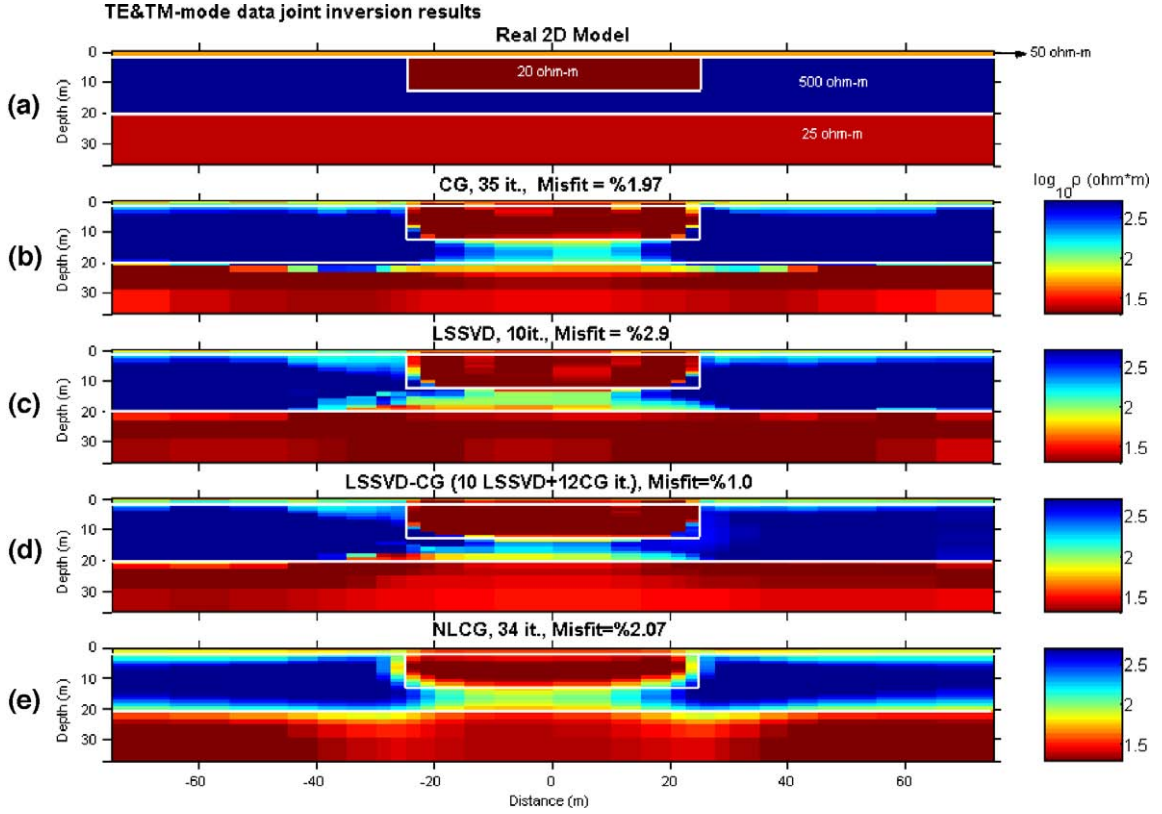

Fig. 1. (a) 2D resistivity model representing a waste-site. The background is a three-layered model with resistivities equal to 50, 500, and 25 Ω m. The thickness of the first and the second layer are 2 and 20 m, respectively. One conductive body with a 20 Ω m resistivity is buried in the second layer between 3–13 m depth and 50–100 m in profile direction. Estimated models obtained from (b) the CG solution, (c) the LSSVD solution, (d) the LSSVD_CG solution, and (e) the NLCG solution. White solid lines indicate the actual model boundaries in this and the following figures.

that the LSSVD_CG algorithm gives a better resolution than the NLCG algorithm.

4.2. Second model

Newman et al. (2003) generated a 3D data set for the model shown in Fig. (2) using Mackie et al.'s (1994) 3D finite-difference modeling code. This model represents a more complex waste site. The background geology is represented by a three-layer earth model with resistivities of 50, 500, and 25 Ω m, respectively, from top to bottom. The corresponding thicknesses of these layers are assumed to be 2 and 19 m, respectively. The buried waste deposit is modeled by two conductive bodies. Their lateral and depth extensions are shown at the top and bottom of Fig. 2. The data along the *y* axis at −2.5 m were sampled at 40 stations with a 5-m sampling interval. We used frequencies of 20, 70, 140 and 230 kHz in order to study the 3D effects on the 2D inversion results. A 5% Gaussian noise was added to the data before inversion.

The *xy* and *yx* apparent resistivities and the impedance phases are taken as TE-mode and TM-mode data, respectively. The data were inverted jointly using a 200 Ω m homogenous half-space as an initial model (Fig. 3). The α values were selected by using the procedure explained in the previous example. The α was set to 0.81 for the calculated 2D models derived by the CG, LSSVD and LSSVD_CG solutions (Fig. 3b, c and d), while the NLCG solution was found to be 20 for the α (Fig. 3e). None of the methods could completely resolve the geometry of the conductive target. The 20 Ω m structure was only resolved by the LSSVD (Fig. 3c), but the basement could not be resolved even by this technique. The main reason for the poor resolution is the three-dimensionality of the data and the screening effect of the surface conductive layer (Newman et al., 2003).

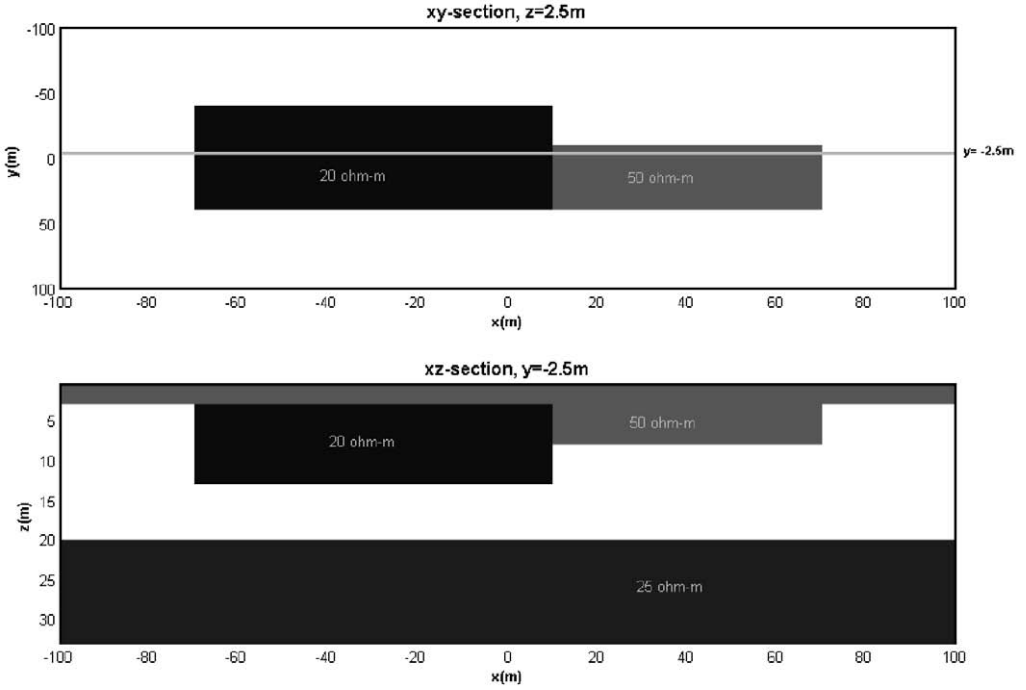

Fig. 2. 3D resistivity model representing a buried waste site. The model consists of a 2-m-thick, 50-Ω m overburden that covers the waste; a 500-Ω m gravel and coarse sand layer of a thickness of 19 m and a lower 25-Ω m basement, representing the conductive tertiary sand, clay, and coal units known to lie beneath the actual waste-site. Two pits with resistivities of 20 and 50 Ω m are buried in the second layer. The lateral and depth extend of the waste pits is shown at the top and bottom of the figures, respectively. Profile $y=-2.5$ m is marked in the *xy* section of the 3D model.

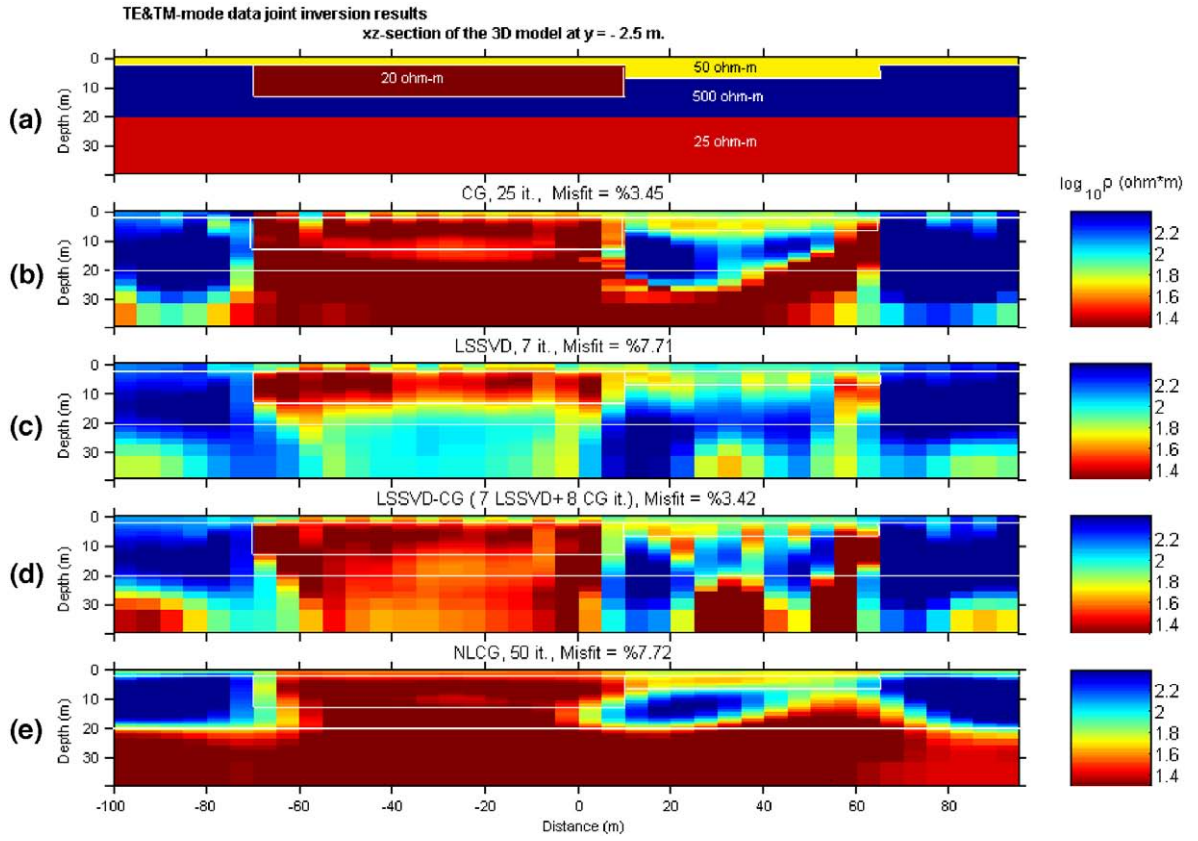

Fig. 3. (a) *xz*-section of the 3D model (Fig. 2) at $y=-2.5$ m; results of the 2D joint inversion of TE- and TM-mode data obtained from the solutions of (b) CG, (c) LSSVD, (d) LSSVD_CG, and (e) NLCG algorithms solution for a 200 Ω m homogenous half-space initial model. (For interpretation of the references to colour in this figure legend, the reader is referred to the web version of this article.)

In general, RMT surveys are carried out on the undisturbed geology and on the buried waste deposits. Therefore, a priori information about the overall resistivity of the host medium is usually available for RMT applications. In the next step we assumed some a priori information about the model. The data were inverted using a two-layer initial model with a 200 Ω m resistivity, a 20-m thick layer at the top, and a 25 Ω m basal conductor. The resistivity of the basement was fixed in all inversion algorithms (Fig. 4). The 2D models were calculated for the same α values as used for the inversion with a homogenous initial model. The estimated models represent the real model much better than the models obtained from inversion with a homogenous half-space initial model. Lateral boundaries between the conductive target and the host medium were resolved, however their vertical boundaries could not be resolved by the CG (uses the L2-norm stabilizer) and NLCG (uses a smoothing stabilizer) algorithms. In addition, they generate some conductive artifacts which are located at distances between 40–70 m along the profile direction, and at a depth between 10–20 m. The LSSVD and LSSVD_CG models resemble the real model more than the other two estimated models. In the estimated model obtained by the LSSVD_CG inversion, the minimum vertical gradient of the blocks between the bottom of the conductive target and the surrounding medium, and the boundary between the second layer and basement, are 2.7 and 4 Ω m/m, respectively. These gradient values are not great enough to resolve boundaries between the resistivity structures.

Newman et al. (2003) also showed that the 2D NLCG inversion of this data could not resolve the

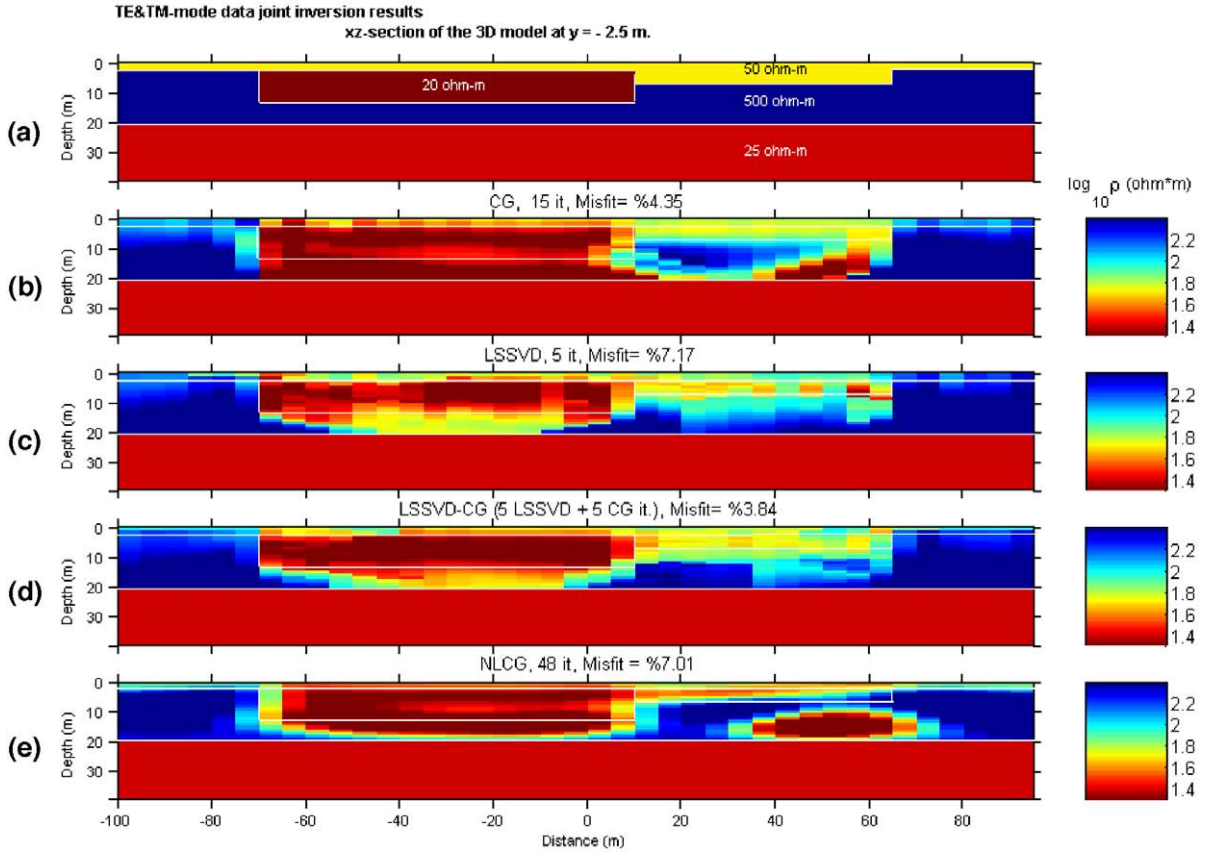

Fig. 4. (a) *xz*-section of 3D model on $y=-2.5$ m; results of the 2D joint inversion of TE- and TM-mode data obtained from the solutions of (b) CG, (c) LSSVD, (d) LSSVD_CG, (e) NLCG algorithms for two-layer initial model.

bottom of the conductive body due to the three-dimensionality of the data. It is well known that TE-mode data are much more affected by the three-dimensionality of the underground structure than TM-mode data (Berdichevsky et al., 1998). Therefore, in the next attempt, only the TM-mode data were now considered in the inversion procedure. The two-layer model, presented in Fig. 4, was used as an initial model in the inversion whereas the resistivity of the basement was fixed during the inversion. Fig. 5 shows the results of all algorithms for the same values, as used for joint data inversion in each of the corresponding algorithms. The bottom of the conductive target was much better derived by the LSSVD_CG and NLCG algorithms. However, lateral and vertical boundaries were found better with the LSSVD_CG algorithm than with the NLCG algorithm (fewer number of iterations and smaller data misfit; 4LSSVD+6CG iteration, misfit=1%). The vertical gradient on the boundary between the conductive target and the surrounding medium is 14.1 Ω m/m if calculated by the LSSVD_CG model, and 10.4 Ω m/m if calculated by the NLCG model.

4.3. Summary of inversion results using synthetic data

The main aim of modeling with synthetic data was to study the practical aspects of different inversion algorithms used for the interpretation of RMT data.

A typical 2D waste-site model was chosen. In particular, the resolution of the bottom of the highly conductive waste was studied by using different inversion techniques (CG; LSSVD; LSSVD_CG and

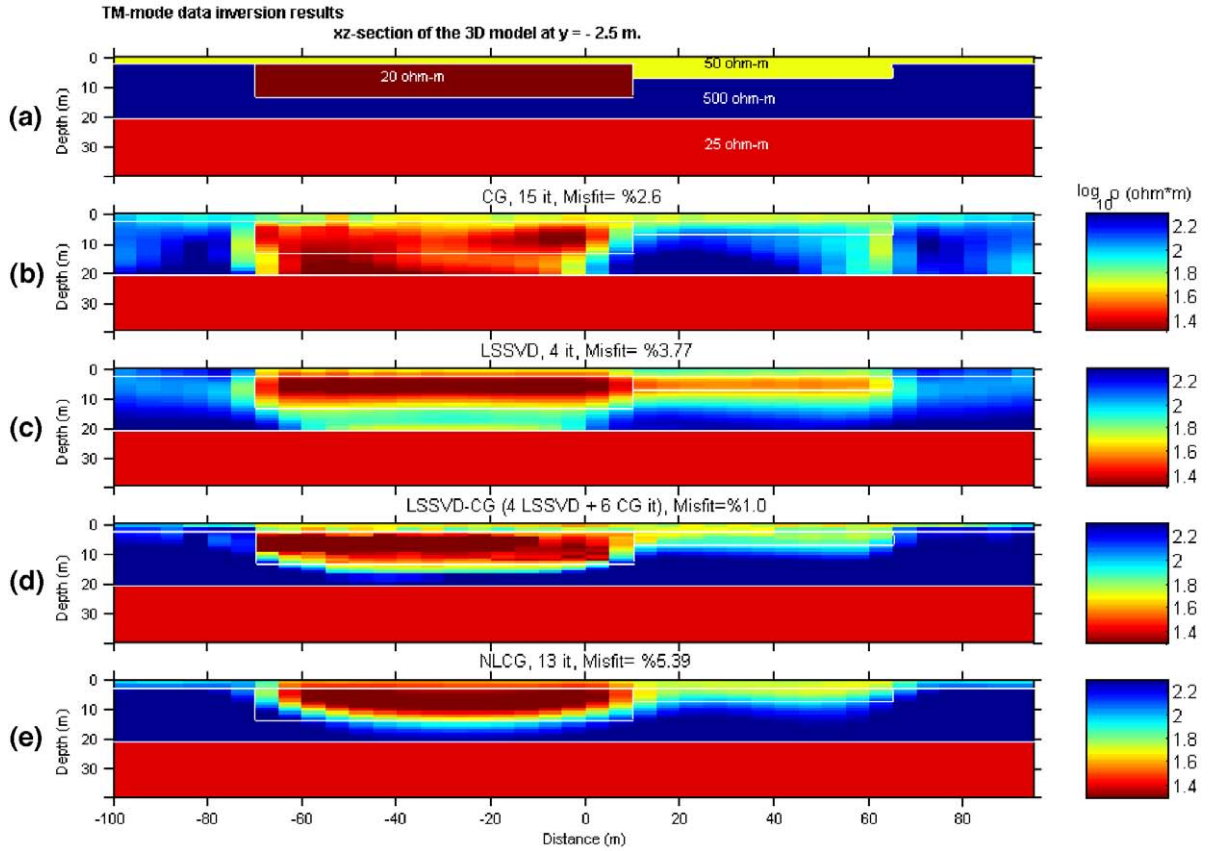

Fig. 5. (a) *xz*-section of 3D model on $y=-2.5$ m; results of the 2D inversion of TM-mode data obtained from the solutions of (b) CG, (c) LSSVD, (d) LSSVD_CG, (e) NLCG algorithms for a two-layered initial model based on the background geology.

NLCG). All inversion techniques could resolve the geometry of the highly conductive waste deposit. However, the best resolution for its bottom was achieved by the LSSVD_CG algorithm, where a maximum vertical gradient of resistivity between the blocks of the highly conductive waste and the surrounding host was achieved.

The model calculations of a 3D waste-site model demonstrate the necessity of a priori information in order to resolve the geometry of the waste site using a 2D inversion and also show that the TM-mode data should be used together with a priori information in the 2D inversion instead of the joint inversion of TE- and TM-mode data. LSSVD_CG and NLCG algorithms yielded the best results.

These results are important for the interpretation of RMT data observed in typical 3D waste deposits. In the following, the information derived by inversion of the synthetic data is applied to a RMT field data set observed near Cologne, Germany.

5. Inversion of the field data

An RMT survey was carried out on a waste site near Cologne. The site was formerly a pit but is now filled with different kinds of industrial waste and household refuse (Recher, 2002; Newman et al., 2003). Newman et al. (2003) discussed the 3D inversion of the observed RMT data set. They also compared 2D and 3D inversion results for selected profiles, $y=-50$ and 0 m. We have applied LSSVD_CG and NLCG inversion algorithms to the same data sets. Apparent resistivities and phases for

four frequency pairs (f=23.4, 68.9 147.2, 234 kHz for TE mode, and f=19.6, 60 123.7, 207 kHz for TM mode) – observed at 31 RMT stations on the profile $y=-50$ m, and at 37 RMT stations on the profile $y=0$ m – were used in the inversion with a station interval of 10 m in the assumed TE-and TM-polarization directions. No stations were available between 350 and 430 m of profile $y=-50$, and between 300 and 410 m of profile $y=0$.

Newman et al. (2003) showed that the 2D NLCG inversion of the selected data could not delimit the bottom of the contaminated area. A 200 Ω m homogenous half-space was used as an initial model for all inversion calculations. We inverted TE-and TM-mode data jointly using the same initial model with the LSSVD_CG (Fig. 6a and c) and NLCG (Fig. 6b and d) algorithms for the same lines ($y=-50$ and 0 m). The regularization parameter α was determined to be 0.69 for the LSSVD_CG algorithm (cooling approximation), and 20 for the NLCG algorithm. The base of the conductive pit was detected below a depth of 18 m. The conductive basement beneath the depth of 20 m could not be resolved by any of the models. This depth appears to be overestimated because borehole data and 3D data inversion of the whole data set (Newman et al., 2003) indicate that the bottom of the pit is at approximately 13-m depth. These results are valid for different regularization parameters used in the NLCG inversions; all models show the same extension of the highly conducting structure below the base of the pit. These results confirm the results of Newman et al. (2003). On the other hand, the LSSVD_CG model looks much more disturbed than the NLCG model because it uses the L2-norm stabilizer which is much more affected by data

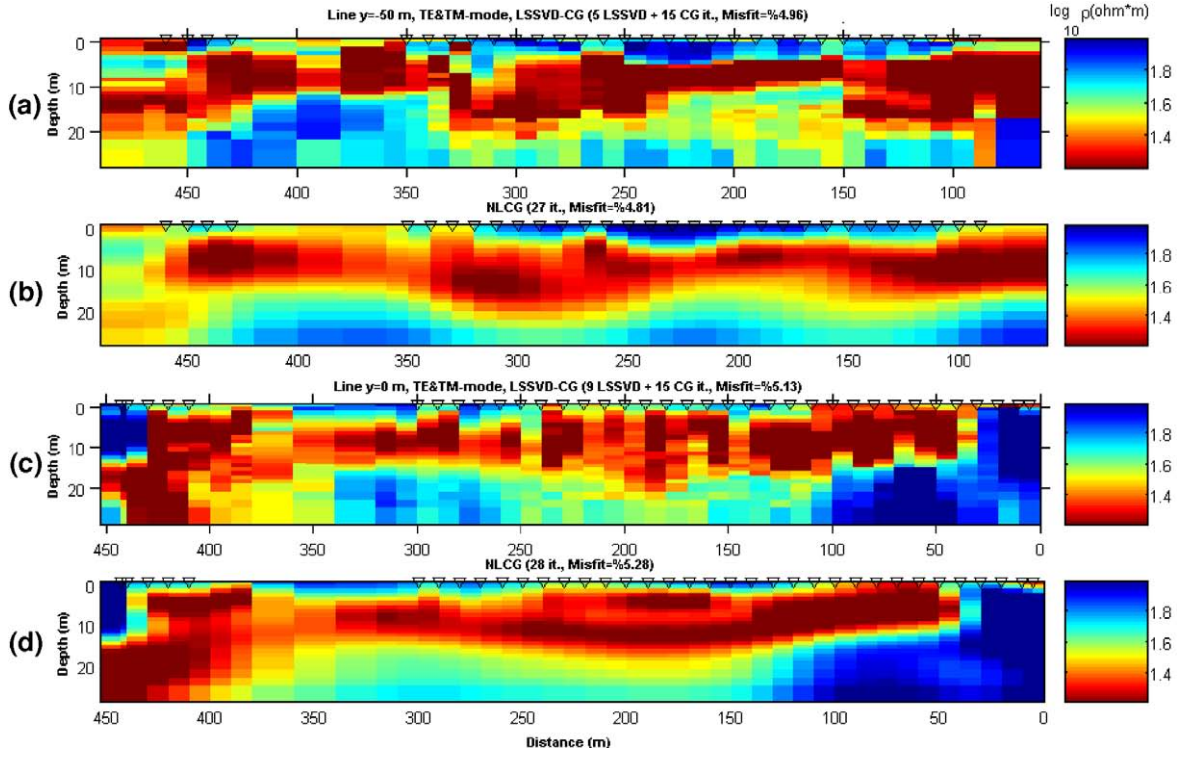

Fig. 6. Results of the 2D joint inversion of TE- and TM-mode field data measured along the line, $y=-50$ m; (a) LSSVD_CG, (b) NLCG solutions and $y=0$ m; (c) LSSVD_CG and (d) NLCG solutions for a 200 Ω m half-space homogenous initial model. The stations locations are shown as down-triangular symbol on the estimated models in these figures and the following figures.

error than the smoothing stabilizer used in NLCG algorithm. However, the LSSVD_CG model should be preferred because it resolves very well the boundaries between resistivity structures.

Considering the synthetic data inversion, TM-mode data were inverted for the same lines and the same initial model was used in the synthetic modeling (Recher, 2002). The basal half-space resistivity is fixed in the inversion. The results of the inversion made by the LSSVD_CG and NLCG algorithms are shown in Fig. 7a, b for line $y=-50$ m, and Fig. 7c, d for line $y=0$ m. The same α values that were used for joint inversion of the field data were used in each corresponding algorithms solution. In models obtained from the LSSVD_CG inversion (Fig. 7a and c), the base of the pit lies at approximately 13-m depth ($\rho<30$ Ω m). On the other hand, its base lies at 15-m depth in models from the NLCG algorithm (Fig. 7b and d). The LSSVD_CG solution gives a much sharper image with a lower number of iterations and smaller misfit values. The vertical gradient of resistivity between the bottom of the waste pit and the surrounding medium is approximately 7.5 and 10 Ω m/m for line $y=-50$ m and for line $y=0$ m for both inversion results (LSSVD_CG and NLCG). This result shows that there are no major differences between the estimated models found with the LSSVD_CG and the NLCG algorithm in Fig. 7.

The data fit is acceptable for all models. In Fig. 8, calculated and observed apparent resistivities and phases are shown for the models obtained from the TM-mode data inversion (for the profile, $y=-50$ m) using LSSVD_CG and NLCG algorithms, respectively. Calculated resistivity from the LSSVD_CG and NLCG algorithm results fit well the measured data. However, calculated phase data from the LSSVD_CG algorithm fit the measured

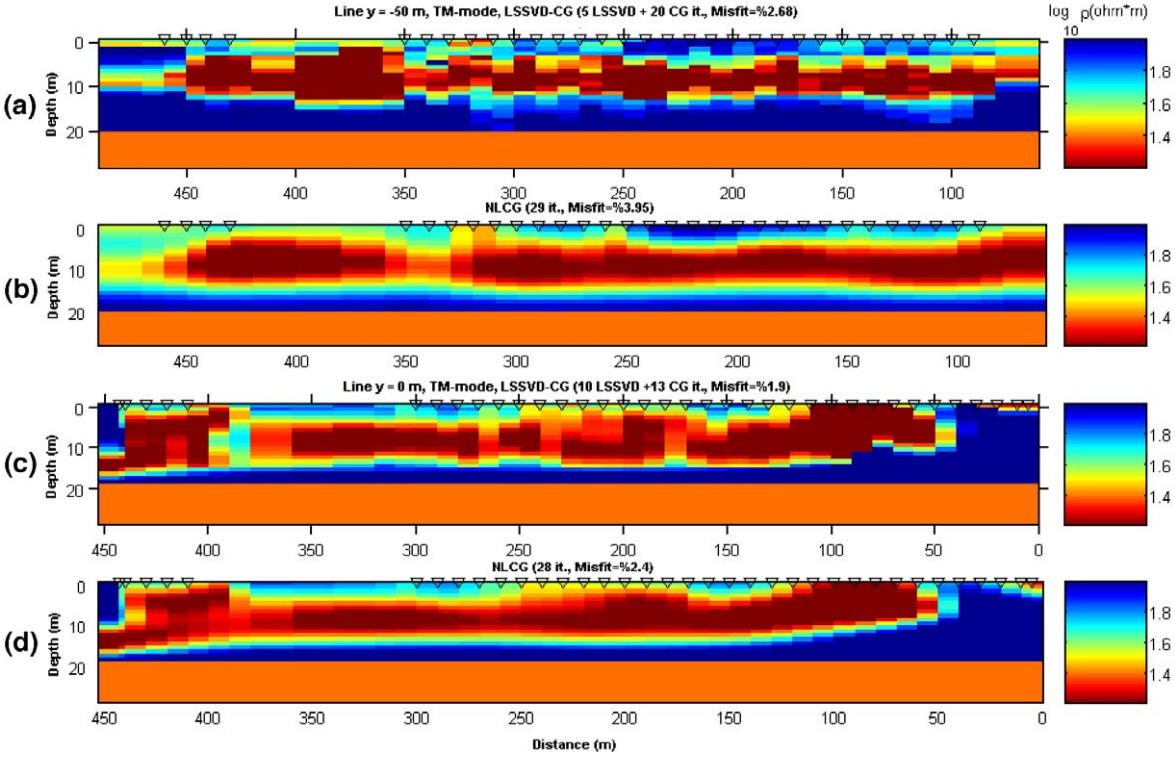

Fig. 7. Results of the inversion of TM-mode field data measured along the line, $y=-50$ m; (a) LSSVD_CG and (b) NLCG and $y=0$ m; (a) LSSVD_CG and (b) NLCG solutions for two-layered initial model based on the background geology.

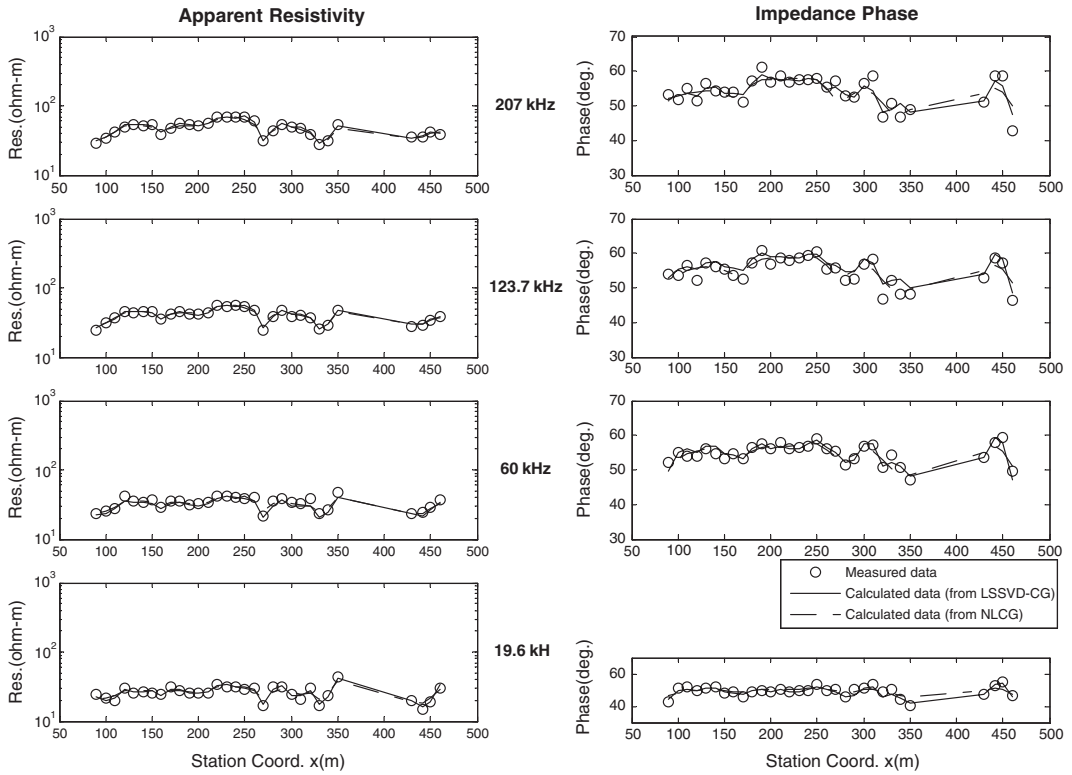

Fig. 8. Comparison between measured data (on line $y=-50$ m) and calculated data from the estimated models shown in c and d obtained from the single TM-mode LSSVD_CG and NLCG inversion, respectively. Symbols mark the observed data, the solid line marks the LSSVD_CG solution and the dash–dot line marks the NLCG solution.

data better than the calculated phase data from the NLCG algorithm.

6. Conclusions

2D inversion continues to play a main role in RMT data interpretation. Based on the results of synthetic data inversion, two conclusions can be drawn:

– as expected, the inversion with the L2-norm stabilizer gives a sharper image than the inversion with the smoothing stabilizer. Results from the inversion of the 2D synthetic data show that the bottom of a waste site can be resolved by using this type of 2D inversion.
– some valuable information can be acquired from 2D inversion of the TM-mode data even though the waste site is 3D. The TM data should be used together with a priori information about the background conductivity structure in the 2D inversion (instead of the joint inversion of the TE and TM mode data) in order to resolve the geometry of the waste site. In particular, the bottom of the waste site can be detected more easily.

The 2D inversion of a RMT field data set, observed on a waste site near Cologne by using different inversion algorithms, confirms some of the results derived by model studies using synthetic data. In order to get a better data fit, we used a two-layered initial model. The basal half-space resistivity is fixed in the synthetic and field data inversions. The basement depth and resistivity of this a priori model can be obtained from the remote reference RMT measurements and/or from borehole samplings.

Acknowledgements

This work was conducted at the University of Cologne and Ankara University. M.E. Candansayar was granted postdoctoral fellowships by TUBITAK (Scientific and Technical Research Council of Turkey) and DFG (Deutsche Forschungsgemeinschaft). The inversion program, R2DMTINV, was developed in the Geosciences Data Processing Laboratory (YEBVIL) of Ankara University under TUBITAK Project No. YDABÇAG-553. Special thanks to Dr. A. Hördt and Dr. M. Bastani who carefully reviewed the paper and gave constructive advice to improve it.

References

Bastani, M., 2001. EnviroMT — a new controlled source radiomagnetotelluric system. PhD thesis, Uppsala University (ISBN 91-554-5051-2).

Bastani, M., Pedersen, L.B., 2001. Estimation of magnetotelluric transfer functions from radiotransmitters. Geophysics 66, 1038–1051.

Baum, A., 1998. Radiomagnetotellurische (RMT) und Georadar-Messungen zur Erkundung einer durch Luftbild im Untergrund vermuteten römischen villa rustica im Wörringer Bruch bei Köln, Master thesis, Institute of Geophysics und Meteorology, University of Cologne.

Beamish, D., 1994. Two-dimensional, regularised inversion of VLF data. J. Appl. Geophys. 32, 357–374.

Beamish, D., 2000. Quantitative 2D VLF data interpretation. J. Appl. Geophys. 45, 33–47.

Berdichevsky, M.N., Dmitriev, V.I., Pozdnjakova, E.E., 1998. On two-dimensional interpretation of magnetotelluric soundings. Geophys. J. Int. 133, 585–606.

Candansayar, M.E., 2002a. Regularized inversion of magnetotelluric data by consequtive use of conjugate gradient and least-squares SVD solvers. PhD. Thesis, Ankara University, Turkey.

Candansayar, M.E., 2002b. Two-dimensional inversion of magnetotelluric data with CG and SVD: a comparisonal study of different stabilizers. SEG International Exposition and Seventy-Second Annual Meeting, Salt Lake City, Utah, Extended Abstract Book, pp. 669–672.

deGroot-Hedlin, C., Constable, S., 1990. Occam's inversion to generate smooth, two-dimensional models from magnetotelluric data. Geophysics 55, 1613–1624.

Farquharson, C.G., Oldenburg, D.W., 1998. Non-linear inversion using general measures of data misfit and model structure. Geophys. J. Int. 134, 213–227.

Farquharson, C.G., Oldenburg, D.W., 2004. A comparison of automatic techniques for estimating the regularization parameter in non-linear inverse problems. Geophys. J. Int. 156, 411–425.

LaBrecque, D.J., Morelli, G., Daily, W., Ramirez, A., Lundegard, P., 1997. Occam's inversion of 3-D electrical resistivity tomography. In: Oristaglio, D.J., Spies (Eds.), Three-Dimensional Electromagnetics. Society of Exploration Geophysicists, pp. 575–590. Publication.

Mackie, R.L., Smith, T.J., Madden, T.R., 1994. Three dimensional electromagnetic modeling using finite difference equations: the magnetotelluric example. Radio Sci. 29, 923–936.

Mackie, R.L., Livelybrooks, D.W., Madden, T., Larsen, J.C., 1997. A magnetotelluric investigation of the San Andreas Fault at Carrizo Plain, California. Geophys. Res. Lett. 24, 1847–1850.

Madden, T.R., 1972. Transmission systems and network analogies to geophysical forward and inverse problems: ONR Technical Report 72-73.

McGillivray, P.R., Oldenburg, D.W., Ellis, R.G., Habashy, T.M., 1994. Calculation of sensitivities for the frequency-domain electromagnetic problem. Geophys. J. Int. 116, 1–4.

McNeill, J.D., Labson, V., 1991. Geological mapping using VLF radio fields. In: Nabighan, M.N. (Ed.), Electromagnetic Methods in Applied Geophysics. Society of Exploration Geophysicists, pp. 521–640. (Chapter 7), publication.

Meju, M., 1994. Geophysical Data Analysis: Understanding Inverse Problem Theory and Practice. Publication of Society and Exploration Geophysicists.

Newman, Hoversten, 2000. Solution strategies for two- and three-dimensional electromagnetic inverse problems. Inverse Probl. 16, 1357–1375.

Newman, G.A., Recher, S., Tezkan, B., Neubauer, F.M., 2003. 3D inversion of a scalar radio magnetotelluric field data set. Geophysics 68, 791–802.

Recher, S., 2002. Dreidimensionale Erkundung von Altlasten mit Radiomagnetotellurik-Vergleiche mit geophysikalisten geochemischen und geologischen Analysen an Bodenproben aus Rammkernsuntresuchungen, PhD thesis, Institute of Geophysics und Meteorology, University of Cologne.

Rodi, W., Mackie, R.L., 2001. Nonlinear conjugate gradients algorithm for 2-D magnetotelluric inversion. Geophysics 66, 174–187.

Sasaki, Y., 1989. Two-dimensional joint inversion of MT and dipole–dipole resistivity data. Geophysics 54, 254–262.

Schmuckher, U., 1987. Substitute conductors for electromagnetic response estimates. PAGEOPH 125, 341–367.

Schröder, R., 1994. Gültigkeitsbereich der 'Ebenen-Wellen-Theorie' unter Berücksichtigung der Verschiebungsströme bezogen auf die geoelektrischen Messmethoden VLF-R (LF-R), CSAMT und short Wave Loop-Loop, Master thesis, Institut für Geophysik und Meteorologie, Universität zu Köln.

Tezkan, B., 1999. A review of environmental application of quasistationary electromagnetic techniques. Surv. Geophys. 20, 279–308.

Tezkan, B., Goldman, M., Greinwald, S., Hördt, A., Müller, I., Neubauer, F.M., Zacher, G., 1996. A joint application of radiomagnetotellurics and transient electromagnetics to the investigation of a waste deposit in Cologne (Germany). J. Appl. Geophys. 34, 199–212.

Tezkan, B., Hördt, A., Gobashy, M., 2000. Two dimensional radio magnetotelluric investigation of industrial and domestic waste sites in Germany. J. Appl. Geophys. 44, 237–256.

Tikhonov, A.N., Arsenin, V.Y., 1977. Solutions to Ill-Posed Problems. John Wiley & Sons, Inc.

Turberg, P., Mueller, I., Flury, F., 1994. Hydrological investigation of porous environments by radio magnetotelluric-resistivity (RMT-R 12-240 kHz). J. Appl. Geophys. 31, 133–143.

Wannamaker, P.E., Stold, J.A., Rijo, L., 1987. A stable finite element solution for 2-D MT modeling. Geophys. J. R. Astron. Soc. 88, 277–296.

Zacher, G., Tezkan, B., Neubauer, F.M., Hoerdt, A., Mueller, I., 1996a. Radio magnetotellurics: a powerful tool for waste-site exploration. Eur. J. Environ. Eng. Geophys. 1, 135–159.

Zacher, G., Tezkan, B., Neubauer,, Zilkens, J., 1996b. Application of radiomagnetotellurics to archaeology-reconstruction of a monastery in Volkenroda (Thuringia) (Extended abstract). EEGS, Nantes, pp. 212–215.

Zhang, A.J., Hobbs, B.A., 1992. Model formulation and model smoothing for 2-D magnetotelluric inversion. Geophys. J. Int. 108, 507–516.

Ziebell, M., 1997. Untersuchung einer Altlast in Köln-Holweide mit Hilfe von RMT und Vergleich verschiedener Interpretationsverfahren. Diplom-thesis, Institut für Geophysik und Meterologie, Universität zu Köln.